Diamond and Carbon Materials (2022)
Clausius Scientific Press, Canada

DOI: 10.23977/dcm.2022.010101
ISSN 2616-3683 Vol. 1 Num. 1

Preparation and Properties of Carbon Nanotubes Based on Graphene Quantum Dots

Xiaohua Bai[1], Hao Jin[2,3], Wenjie Kong[3], Hu Yang[3,*], Yun He[3], Qing Lin[2,3,*]

[1]Nanning College of Technology, Guilin, 541006, China
[2]College of Biomedical Information and Engineering, Hainan Medical University, Haikou, 571199, China
[3]College of Physics and Technology, Guangxi Normal University, Guilin, 541004, China
[*]Corresponding author

Keywords: Graphene, carbon nanotube, Catalytic-free, hybrid materials

Abstract: In this paper, we use a catalyst-free CVD method to prepare carbon nanotubes. In this experiment, the factors affecting the morphology and microstructure of carbon nanotubes during the catalyst-free preparation of carbon nanotubes based on graphene quantum dots were systematically studied. The effects of growth temperature, growth time and acetylene gas flow on the quality of carbon nanotubes were mainly explored.

1. Introduction

Since the discovery of carbon nanotubes in 1991 and the discovery of graphene in 2004 [1,2], due to its excellent electrical, thermal, mechanical and optical properties, it has been widely used in field effect transistors, field emission devices, energy storage materials, composite materials, biological Sensors and other aspects have been widely used. The structure of graphene/carbon nanotubes (G/CNTs) composites determines its excellent physical and chemical properties, which has also attracted the attention of researchers. The reported preparation methods of CNTs usually include arc discharge method, laser ablation method and catalytic chemical vapor deposition method. Although methods for growing CNTs on graphene have been reported, the catalyst-free preparation of carbon nanotubes based on graphene quantum dots is rarely reported. In this paper, we use a catalyst-free CVD method to prepare carbon nanotubes. In this experiment, the factors affecting the morphology and microstructure of carbon nanotubes during the catalyst-free preparation of carbon nanotubes based on graphene quantum dots were systematically studied. The effects of growth temperature, growth time and acetylene gas flow on the quality of carbon nanotubes were mainly explored.

2. Experimental Part

2.1. Sample preparation

2.1.1. Preparation of Carbon Nanotubes Based on Graphene Quantum Dots

Graphene quantum dots (self-made in the laboratory), Ar, C_2H_2, Start the vacuum tube furnace (RF-5301PC), Quartz tube (customized), quartz boat. The schematic diagram of the experimental device is shown in Figure 1.

Figure 1: Schematic diagram of experimental device for carbon nanotube preparation by CVD method

2.1.2. Experimental Procedure

(1) First, 50mg of GQDs samples were weighed and laid flat in quartz boat. Then, we put the quartz boat loaded with GQDs into the quartz tube. Subsequently, the quartz tube was placed in the middle of the vacuum tube furnace. Then, it is necessary to install the Ar tank, C_2H_2 tank, gas flowmeter and quartz tube, and cover the open vacuum tube furnace. The flow rate of Ar introduced is 60 ml/min. Then, the air tightness of the experimental device was checked to ensure that the experimental device did not leak. Ar was introduced into the tubular furnace at a rate of 60 ml/min and kept for more than 20 minutes, so that the residual air in the vent pipe and the container was fully discharged.

(2) The flow rate of argon was adjusted to 80 ml/min.Open the switch and setting button of the tubular furnace, set the heating rate of 10 min/℃, heating temperature, heating time and cooling rate, and then start the operation.

(3) When the temperature rises to the set temperature value (700 ℃, 800 ℃, 900 ℃, 1000 ℃), C_2H_2 is introduced and heated for 5min. The gas flow rate of AR was adjusted to 100 ml/min in order to discharge the C_2H_2 in the quartz tube out of the tube,After 10 min, the gas flow of AR was adjusted to 50 ml/min, CNTs samples were collected after the samples were naturally cooled to room temperature. Respectively recorded as: CNTs-700, CNTs-800, CNTs-900, CNTs-1000. Where the number indicates the heating temperature, and the unit is centigrade.

2.2. Characterization of Samples

The morphology and structure of carbon nanotubes were observed by field emission scanning electron microscope (Hitachi SU8010) and field emission transmission electron microscope (FEI Tecnai G2 F20). Raman spectra of carbon nanotubes were analyzed using a Raman spectrometer (LabRAMm HR Evolution). Fourier transform infrared spectrometer (Spectrum Two) was used to analyze the infrared spectral characteristics of the samples; XPS analysis of carbon nanotubes was performed by X-ray photoelectron spectroscopy (ESCALAB 250Xi); The photoluminescence spectra

of carbon nanotubes were measured using a fluorescence spectrophotometer (RF-5301pc).

3. Experimental Results and Analysis

In order to obtain satisfactory products, we try to change different heating temperature, growth time and gas flow rate for comparative experiments. The experimental results are as follows.

3.1. Effect of Growth Temperature on Morphology and Microstructure of Samples

According to the above experimental methods, the growth temperature was changed to explore the effect of temperature on the morphology and microstructure of the samples.The growth time was 5min, the acetylene gas flow rate was 0.25 ml/min, and the growth temperature was 700 ℃, 800 ℃, 900 ℃, and 1000 ℃. The experiment was repeated.Collect the samples after the tube furnace is naturally cooled to room temperature, and mark the obtained samples as cnts-700, cnts-800, cnts-900 and cnts-1000, where the number indicates the heating temperature, and the unit is centigrade.

3.1.1. Morphology Analysis of Samples

3.1.1.1 Scanning Electron Microscope (SEM) Analysis

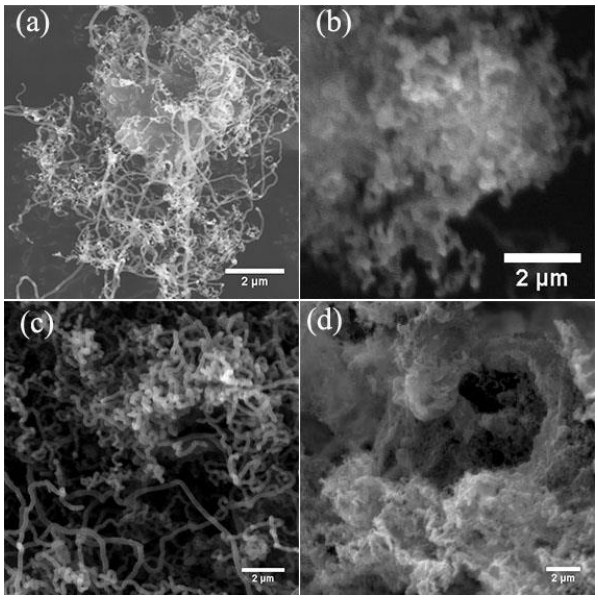

(a) CNTs-700, (b) CNTs-800, (c) CNTs-900, (d) CNTs-1000,of students doing part of the test independently

Figure 2: Effect of different growth temperatures on the morphology of CNTs SEM image

The influence of different growth temperatures on the morphology of carbon nanotubes is shown in Figure 2. It can be seen from Figure 2 (a) that CNTs are arranged in a disorderly manner and bent at will, and the diameter of CNTs is distributed between 30-80 nm, with a large distribution range. Figure 2 (b) shows that CNTs are also intertwined, but the diameter distribution is relatively uniform. Compared with Figures 2 (a) and (b), it can be clearly seen in Figure 2 (c) that the number of carbon nanotubes obtained by increasing the growth temperature is increased, the diameter of CNTs is increased, and the distribution is more uniform, which is in the range of 80-100 nm. As can be seen from Figure (d), when the temperature continues to rise to 1000 ℃, a small amount of carbon nanotubes are generated, and a large amount of deposited carbon is generated. According to the

comprehensive analysis of SEM, the growth temperature has a significant effect on the morphology of carbon nanotubes. When the growth temperature is lower than 900 ℃, the reason for the growth of a small amount of CNTs is that the low temperature can not effectively cleave acetylene, and there is not enough carbon source, thus affecting the growth of CNTs. High quality CNTs cannot be grown at high temperature because carbon atoms generated at high temperature are deposited on the surface of graphene quantum dots, forming deposited carbon, which is not conducive to the growth of carbon nanotubes. When the growth temperature is 900 ℃, it is more suitable for the growth of carbon nanotubes, and the quality of carbon nanotubes is the best.

3.1.1.2 Transmission Electron Microscopy (TEM) Analysis

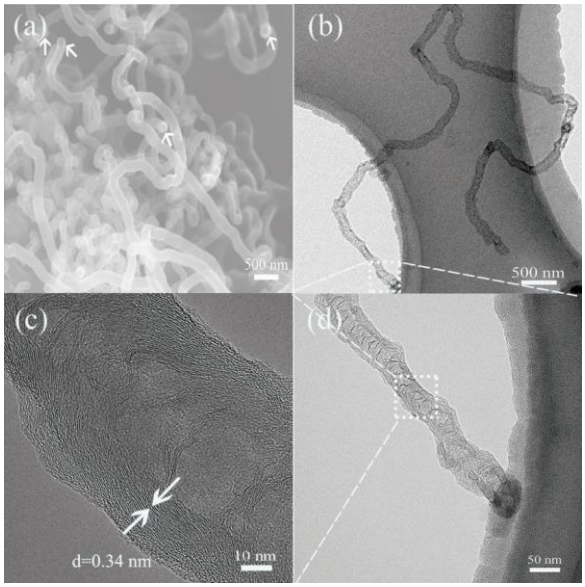

Figure 3: SEM (a) and TEM (b), (c) and (d) of CNTs-900 sample

Figure 3 shows the SEM (a) and TEM (b), (c) and (d) of carbon nanotubes prepared at 900 ℃. It can be clearly seen from Figure 3 (a) that the diameter of CNTs is about 80-100 nm, and the length is several microns, which is relatively uniform. In addition, as shown by the white arrows in Figure 3 (a), CNTs present unique nozzles, indicating that they are carbon nanotubes rather than carbon nanofibers. Interestingly, Figures 3 (b) and (d) show that the samples are mainly spiral carbon nanotubes, with an obvious bamboo shape appearance. In other words, the carbon nanotubes obtained by the CVD method without metal catalyst based on graphene quantum dots in this experimental system are bamboo carbon nanotubes (BCNTs). As shown in the high-resolution TEM (HRTEM) image of Figure 3 (c), the tube walls of BCNTs are composed of distinct bends and clearly visible single compartments. Generally, the graphite layer is not arranged parallel to the axis of the tube. In addition, it can be clearly seen in Figure 3 (c) that BCNTs have a multi wall structure and a clear lattice stripe structure, so they belong to carbon materials. The lattice stripe spacing is about 0.34 nm, which is almost the same as that of ordinary CNTs.

3.1.1.3 Raman Analysis

Figure 4 shows the Raman spectra of CNTs samples at different growth temperatures. It can be seen from the Figure that CNTs have D peak and G peak at 1353 cm-1 and 1587cm-1 respectively, which are characteristic peaks of typical graphite materials or carbon nanotubes [3]. Among them, the D peak represents internal defects and edge effects, and the G peak represents sp2 hybrid carbon

atoms [4]. The disorder of carbon based nanomaterials is usually represented by the intensity ratio (ID/IG) of the D peak to the G peak [5,9]. The ID/IG ratio close to 0 indicates high crystallinity, and close to 1 indicates that CNTs have high disorder [6]. By calculation, the ID/IG ratios of BCNTs-700, BCNTs-800 and BCNTs-900 were 0.89, 0.95 and 0.97, respectively.The results show that the obtained BCNTs are disordered with prominent edge plane positions [6].

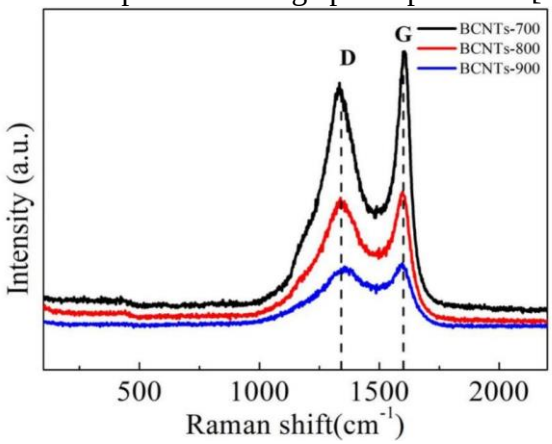

Figure 4: Raman spectra of CNTs prepared at different growth temperatures

3.1.1.4 Fourier Transform Infrared Spectroscopy (FTIR) Analysis

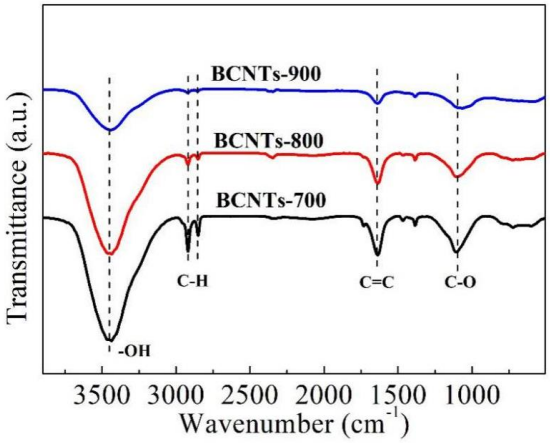

Figure 5: FTIR spectra of CNTs prepared at different growth temperatures

As shown in Figure 5, FTIR analysis can be used to determine and characterize the surface functional groups of BCNT samples. It can be seen that all BCNTs have an obvious infrared absorption peak at 3453 cm-1, which is the characteristic absorption band of -OH stretching vibration [7]. Obviously, these absorption peaks gradually decrease with increasing annealing temperature. In addition, two weak absorption peaks of BCNTs can be seen near 2924 cm-1 and 2853 cm-1, which are caused by C-H stretching vibrations [7,8]. The two bands at 1648 cm-1 and 1102cm-1 are due to the C=C stretching vibration and the C-O stretching in the -OOH group, respectively [9]. The results show that BCNTs contain a variety of oxygen-containing functional groups, and these absorption peaks gradually decrease with increasing annealing temperature.

3.1.1.5 X-ray Photoelectron Spectroscopy (XPS) Analysis

The contents of carbon and oxygen in the BCNTs samples, as well as the binding energy of carbon and oxygen, were detected by X-ray photoelectron spectroscopy. As shown in Figure 6 (a), all

BCNTs have a strong C 1s (284.7 eV) peak and a weak O 1s (532.08 eV) peak. To obtain information on oxygen-containing functional groups in BCNTs, we performed a fine scan of the C1s spectrum, decomposing each C1s peak into 4 peaks. As shown in Figure 6(b), the main peak at 284.7 eV is graphitized sp2 carbon atom (C=C), the rest are hydroxyl (C-O bond), carbonyl (C=O) and carboxyl (O-C=O), the positions are respectively at 286.0, 287.8 and 288.9 eV [11].

According to the test results of XPS, the detailed information of carbon and oxygen-containing functional group contents of BCNTs can be obtained from Table 1. The results show that BCNTS has high carbon content (>88.12%) and low oxygen content (<11.22%). Notably, with increasing growth temperature, the C-O content of BCNTS-700 is 7.70%, while the C-O content of BCNTS-900 is 7.16%, which indicates the higher thermal stability of C-O. However, the contents of C=O and O-C=O were significantly reduced.

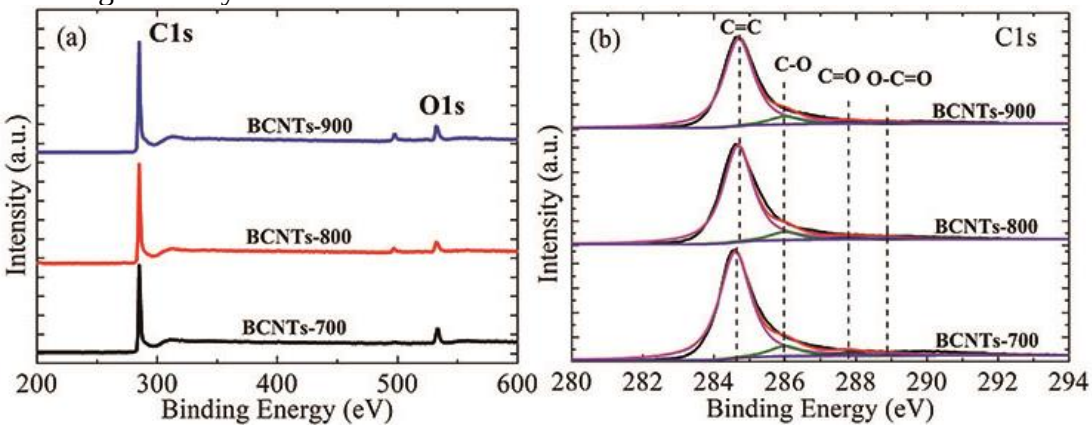

Figure 6: (a) XPS spectra of CNTs prepared at different growth temperatures; (b) C1s spectra of CNTs

Table 1: Contents of C, O, C=C, C-O, C=O, C-C=O of CNTs

samples	C=C	C-O	C=O	C-C=O	C	O
BCNTs-700	74.81	7.70	3.08	2.52	88.12	11.22
BCNTs-800	80.29	7.18	1.97	1.70	91.12	8.08
BCNTs-900	80.26	7.16	1.66	1.60	91.13	8.24

It is well known that carbon nanotubes are usually prepared under the catalysis of metal catalysts. However, in this experiment, BCNTs were synthesized only by annealing GQDs in an Ar/C2H2 atmosphere. The results show that graphene oxide with more oxygen content has higher catalytic activity. Defining the oxygen content of the sample as 100%, the GQDs are oxygen-rich with a high oxygen content of about 53.7% [12]. The formation of BCNTs is thought to be related to the catalytic activity of GQDs. That is to say, when the annealing temperature exceeds 700 ℃, most of the oxygen-containing functional groups of GQDs are decomposed into CO, CO2, or H2O, and there will be many high-energy unsaturated carbon dangling bonds in GQDs. These unsaturated carbon dangling bonds are active sites, and these unsaturated carbon dangling bonds have high catalytic activity for the decomposition of C2H2 into carbon and hydrogen. Therefore, the decomposed carbon diffuses and self-assembles to form BCNTs.

3.2. The Effect of Growth Time on the Morphology and Microstructure of the Samples

According to the experimental method described in "Experimental Procedure", change the growth time to explore the effect of growth time on the morphology and microstructure of the sample. The

growth temperature was set to 900 ℃, the flow rate of acetylene gas was 0.25 ml/min, and the growth time was 5 min, 25 min, 45 min, and 65 min, respectively, and the experiment was repeated. After the tube furnace was naturally cooled to room temperature, the samples were collected, and the obtained samples were labeled as CNTs-5, CNTs-25, CNTs-45, and CNTs-65, where the numbers represent the growth time in minutes.

3.2.1. Morphology Analysis of Samples

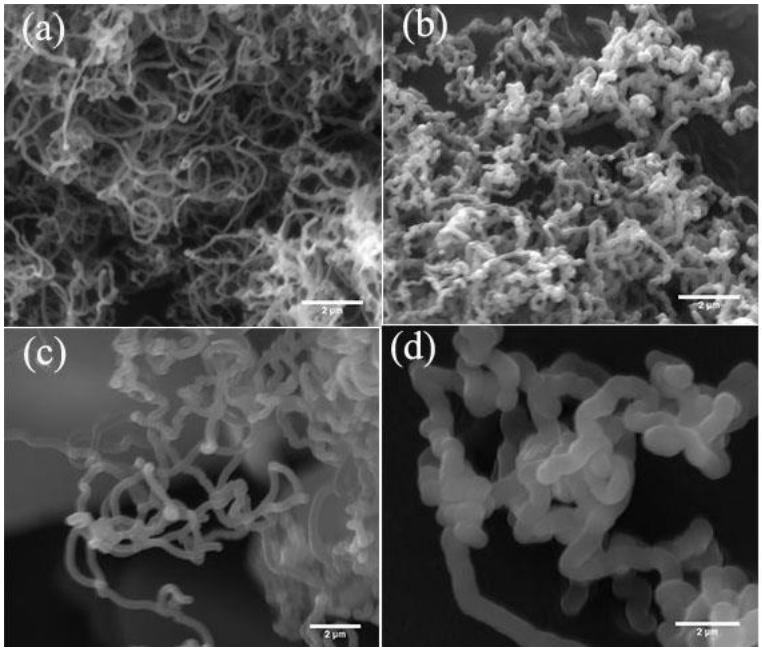

(a) 5 min, (b) 25 min, (c) 45 min, (d) 65 min

Figure 7: SEM images of the effect of different growth times on the morphology of CNTs

The SEM images of the effect of different growth times on the morphology of carbon nanotubes are shown in Figure 7. It is observed from Figure 7 (a) that the CNTs have uniform tube diameters ranging from 80-100 nm. It can be seen from Figure 7 (b) that the CNTs are intertwined with each other, bend at will, the tube diameter has increased, the distribution range is wide, about 100-150 nm, and the long diameter of the carbon nanometers is shortened. When the growth time continued to increase to 45 min, the winding situation of the obtained CNTs-45 samples changed, the number decreased, and the tube diameter also increased, about 280-300 nm. It can be observed from Figure (d) that the CNTs-65 has the largest diameter and is distributed at 650-700 nm. From the comprehensive analysis of SEM, it can be obtained that within a certain time range, with the increase of growth time, the diameter of CNTs increases, that is, the growth time has a greater impact on the diameter of the prepared carbon nanotubes, but the growth time The basic morphology of carbon nanotubes will not be changed.

3.2.2. Raman Spectroscopy (Raman) Analysis

Figure 8 is the Raman pattern of CNTs samples with different growth time. It can be seen from the Figure that all CNTs samples have D peaks and G peaks in the range of 1333-1354 cm-1 and 1587-1897 cm-1, which are characteristic peaks of typical graphite materials or carbon nanotubes [3]. Among them, the D peak represents internal defects and edge effects, and the G peak represents sp2 hybridized carbon atoms [4]. The prepared carbon nanotube samples showed D peaks and G peaks, which proves that the samples have a certain amount of defects and a large number of sp2 hybridized

carbon atoms. The disorder of carbon-based nanomaterials is usually expressed by the intensity ratio of D peak to G peak(ID/IG). The ID/IG ratio close to 0 indicates higher crystallinity, and close to 1 indicates that the CNTs[6] are highly disordered. It can be obtained by calculation that the ID/IG ratio (0.93-0.98) of all CNTs samples is higher than that of GQDs (0.81) [12], indicating that after growing CNTs, the material is disordered and the overall disorder is enhanced.

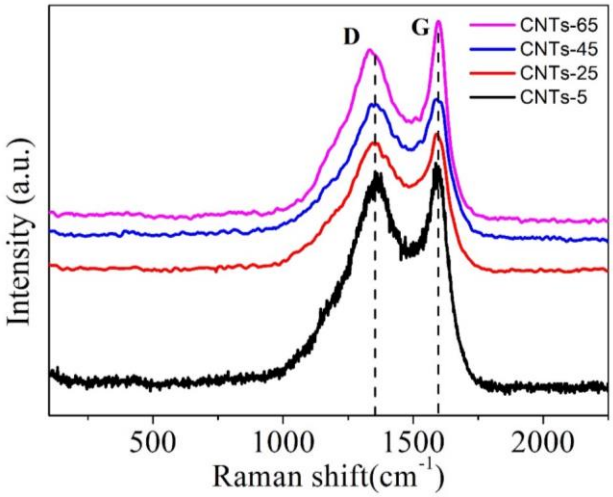

Figure 8: Raman spectra of CNTs prepared under different growth times

3.2.3. Fourier Transform Infrared Spectroscopy (FTIR) Analysis

Figure 9 shows the Fourier transform infrared spectra of CNTs prepared under different growth times. According to this figure, the functional groups on the surface of CNTs samples can be analyzed and determined. The Figure shows that all CNTs have obvious infrared absorption peaks at 3451-3453 cm-1, which is caused by -OH stretching vibration [7]. In addition, around 2915 cm-1 and 2853 cm-1, two faint absorption peaks of CNTs induced by C-H stretching vibration can be seen [11]. The two bands at 1612-1648 cm-1 and 1102 cm-1 are due to the C=C stretching vibration and the C-O stretching in the -OOH group, respectively [12]. The results show that CNTs contain a variety of oxygen-containing functional groups. Compared with all samples, the absorption peak of CNTs-5 is the weakest, which is the result of the effect of the generated carbon nanotubes.

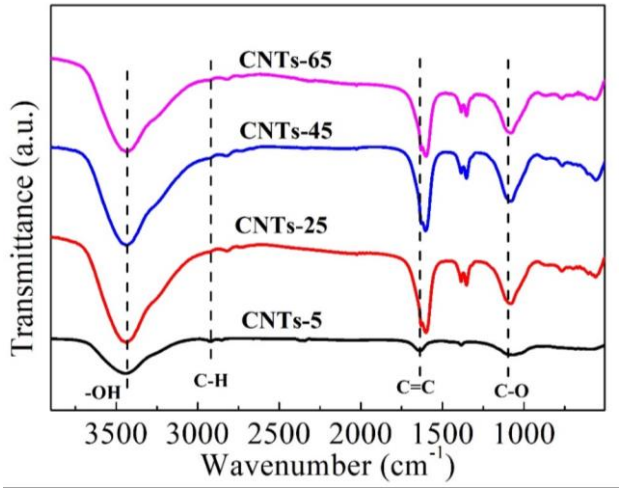

Figure 9: FTIR spectra of CNTs prepared at different growth time

3.2.4 X-ray Photoelectron Spectroscopy (XPS) Analysis

The content of carbon and oxygen in the CNTs samples and the binding energy of carbon and oxygen were detected by X-ray photoelectron spectroscopy. It can be clearly seen from Figure 10(a) that all CNTs have a strong C 1s (284.7 eV) peak and a weak O 1s (532.08 eV) peak. To obtain information on oxygen-containing functional groups in the samples, we decomposed each C 1s peak into 4 peaks. As shown in Figure 10(b), the main peak at 284.7 eV is graphitized sp2 carbon atom (C=C), and the rest are C-O bond, C=O bond and O-C=O bond, respectively, at 286.0, 287.8 and 288.9 eV [11]. According to the XPS results, the CNTs carbon and oxygen-containing functional group contents can be obtained from Table 2. We define the O content of the sample as 100%. The results showed that CNTS had higher carbon content (>91.11%) and lower oxygen content (<6.03%) with increasing growth time. With the increase of growth time, the C-O content of carbon nanotubes increased first and then decreased, from 7.16% of sample CNTs-5 to 10.85% of sample CNTs-45, and then decreased to CNTs-65 (7.37%), but the contents of C=O and O-C=O remained relatively stable, and the contents were relatively reduced.

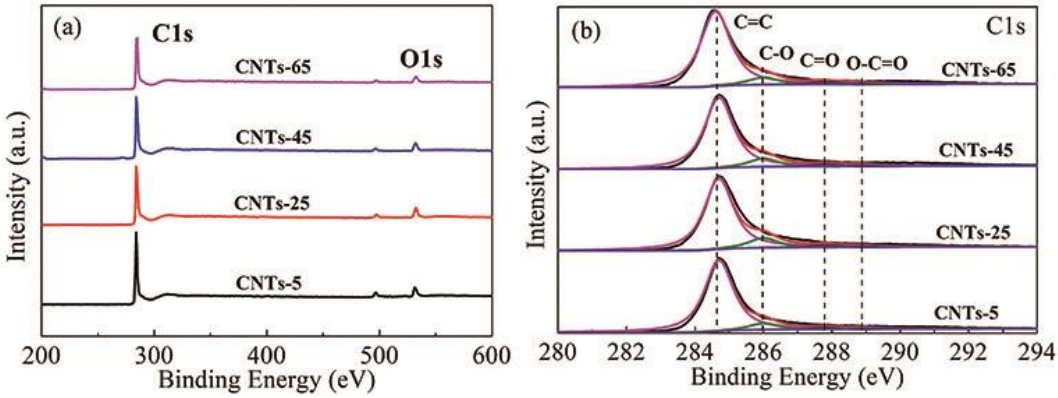

Figure 10: (a) XPS spectra of CNTs prepared with different growth times; (b) C1s spectra of CNTs

Table 2: Contents of C, O, C=C, C-O, C=O, C-C=O of CNTs

samples	C=C	C-O	C=O	C-C=O	C	O
CNTs-25	80.26	7.16	1.66	1.60	91.13	8.24
CNTs-25	77.77	9.16	2.22	1.96	91.11	8.09
CNTs-45	78.05	10.85	2.29	1.22	92.40	6.83
CNTs-65	82.37	7.38	1.93	1.60	93.28	6.03

It is well known that GQDs are oxygen-rich with a high oxygen content of about 53.7% [12]. The formation of CNTs is thought to be related to the catalytic activity of GQDs. That is to say, at temperatures above 700 ℃, most of the oxygen-containing functional groups of GQDs are decomposed into CO, CO_2, or H_2O, and there will be many high-energy unsaturated carbon dangling bonds in GQDs. These unsaturated carbon dangling bonds are active sites and have high catalytic activity for the decomposition of C_2H_2 into carbon and hydrogen. Therefore, the decomposed carbon diffuses and self-assembles to form CNTs. Based on the results, we guessed that when the temperature was 900 ℃, as the growth time increased, the more carbon and hydrogen were decomposed by C_2H_2. When the growth time was 5 min, the decomposed carbon diffused and self-assembled to form CNTs reaching saturation. If the growth time is prolonged, it will be unfavorable for the synthesis of CNTs.

3.3. Effect of Acetylene Gas Flow on Morphology and Microstructure of Samples

According to the experimental method described in "Experimental Procedure", the flow rate of acetylene gas was changed to explore the effect of acetylene flow rate on the morphology and microstructure of the sample. We set the growth temperature to 900 ℃, the growth time of 5 min, and the acetylene gas flow rates of 0.25 ml/min, 1.5 ml/min, 2.5 ml/min, and 3.5 ml/min, respectively, and repeated the experiment. After the tube furnace was naturally cooled to room temperature, the samples were collected, and the obtained samples were labeled as CNTs-0.25, CNTs-1.5, CNTs-2.5, and CNTs-3.5, where the numbers indicated the flow rate of acetylene gas, in milliliters per minute.

3.3.1 Morphology Analysis of Samples

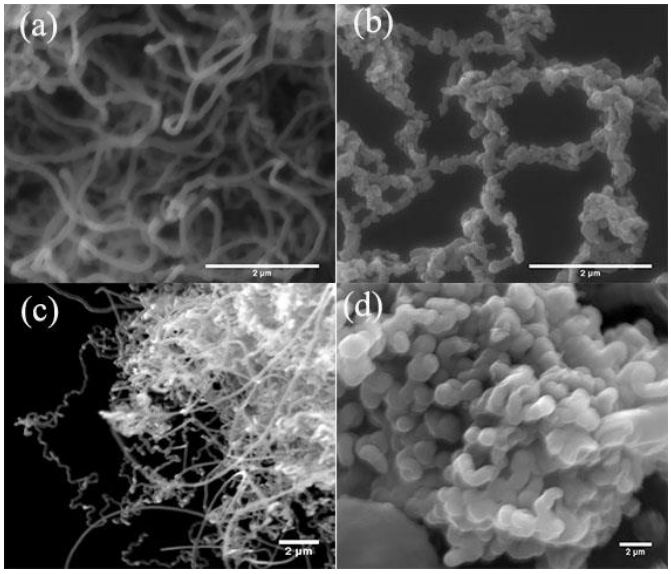

(a) CNTs-0.25, (b) CNTs-1.5, (c) CNTs-2.5, (d) CNTs-3.5

Figure 11: SEM images of the effect of different C2H2 flow rates on the morphology of CNTs

The SEM images of the effect of different growth temperatures on the morphology of carbon nanotubes are shown in Figure 11. By observing Figure 11, it can be seen that the shape of the CNTs of the CNTs-1.5, CNTs-2.5 and CNTs-3.5 samples changed greatly. The CNTs of the CNTs-0.25 sample in Figure 11 (a) have a small diameter (80-100 nm), a relatively uniform distribution, and are all long tubes. It can be clearly seen from the Figure 11 (b) that the CNTs are intertwined and twisted into a network structure, and the length and diameter of the tube become smaller. It can be seen from the pictures 11 (c) and (d) that the entanglement of carbon nanotubes is more serious, and the surface becomes rougher, and the diameter of the tube increases significantly, which are distributed at 140-230 nm and 450-500 nm, respectively. It can be seen from the comprehensive analysis of SEM that the flow rate of acetylene gas has a significant effect on the morphology of the prepared carbon nanotubes. When the acetylene flow rate was 0.25 ml/min, the quality of the prepared carbon nanotubes was better.

3.3.2 Raman Spectroscopy (Raman) Analysis

Figure 12 is the Raman spectrum of CNTs samples with different growth temperatures. It can be seen from the Figure that all CNTs have D peak and G peak, which is the Raman spectrum of typical carbon materials [3]. The D peaks and G peaks are in the range of 1333-1353 cm-1 and 1587-1593 cm-1. Among them, the D peak represents internal defects and edge effects, and the G peak represents

sp2 hybridized carbon atoms [4]. There are D peaks and G peaks in the CNTs samples, which proves that the samples have a certain amount of defects and a large number of sp2 hybrid carbon atoms. In particular, the D peaks and G peaks of CNTs-2.5 and CNTs-3.5 are broadened and the intensity is weakened, indicating the increase of disorder and defects. The intensity ratio of D peak to G peak (ID/IG) is usually used to represent the disorder of carbon-based nanomaterials [9]. The larger the ID/IG ratio is, the more CNTs have defects and are highly disordered [6]. It can be known from the calculation that the ID/IG ratios of CNTs-0.25, CNTs-1.5, CNTs-2.5 and CNTs-3.5 are 0.97, 0.92, 0.97 and 0.98, respectively. It was shown that the obtained CNTs were disordered [10-11], and all had significant edge plane positions [6]. The order of carbon nanotubes with network structure is strong.

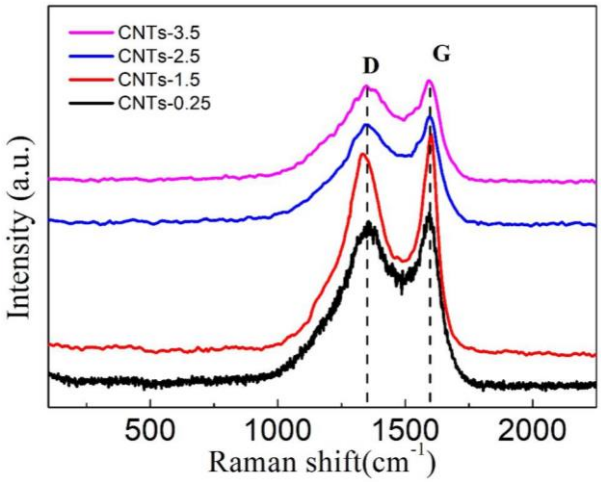

Figure 12: Raman spectra of CNTs prepared with different C2H2 fluxes

3.3.3 Fourier Transform Infrared Spectroscopy (FTIR) Analysis

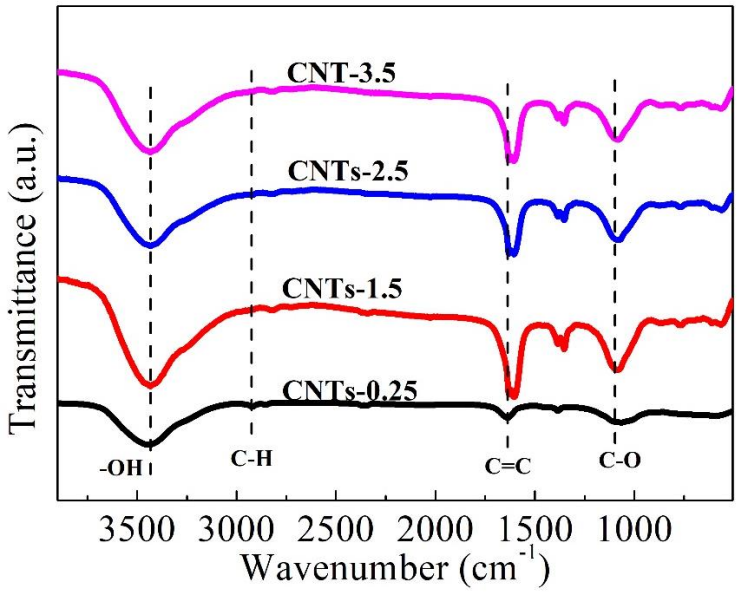

Figure 13: FTIR spectra of CNTs prepared with different C2H2 fluxes

Figure 13 shows the FTIR spectra of CNTs prepared with different C2H2 gas flow rates. FTIR analysis was used to characterize and determine the surface functional groups of CNTs samples. It can be seen that all CNTs have obvious infrared absorption peaks at 3451-3453 cm-1, which is the characteristic absorption band of -OH stretching vibration [7]. Obviously, with the increase of

acetylene flow, the absorption peak of CNTs-0.25 is the smallest. In addition, around 2924 cm-1 and 2853 cm-1, two faint absorption peaks of CNTs induced by C-H stretching vibration can be seen [7,8]. The two bands at 1612-1648 cm-1 and 1102 cm-1 are due to the C=C stretching vibration and the C-O stretching in the -OOH group, respectively [9,10]. The results show that CNTs contain a variety of oxygen-containing functional groups. Compared with all samples, the absorption peak of CNTs-0.25 is the weakest, which may be the result of the effect of generating a large number of CNTs.

3.3.4 X-ray Photoelectron Spectroscopy (XPS) Analysis

Figure 14 shows the XPS spectra (a) and C1s spectra (b) of CNTs prepared at different growth temperatures. X-ray photoelectron spectroscopy was used to detect the content of carbon and oxygen in the CNTs samples, as well as the binding energy of carbon and oxygen. As shown in Figure 14 (a), all CNTs have a strong peak of C 1s (284.7 eV) and a weak peak of O 1s (532.08 eV). To obtain information on oxygen-containing functional groups in CNTs, we performed a fine scan of the C1s spectrum, decomposing each C1s peak into 4 peaks. As shown in Figure 14(b), the main peak at 284.7 eV is the graphitizedsp2 carbon atom (C=C), and the rest are C-O bonds, C=O bonds and O-C=O bonds, at 286.0, 287.8 and 288.9 eV, respectively [9-10]. As can be seen from Table 3, CNTS has high carbon content (>87.74%) and low oxygen content (<7.54%). With the increase of acetylene flow rate, the carbon content and C=C bond content show a decreasing trend, and compared with other samples, the CNTs-0.25 sample has the lowest C-O content (7.16%) C=O and O-C=O The content corresponds to the FTIR spectrum of the sample.

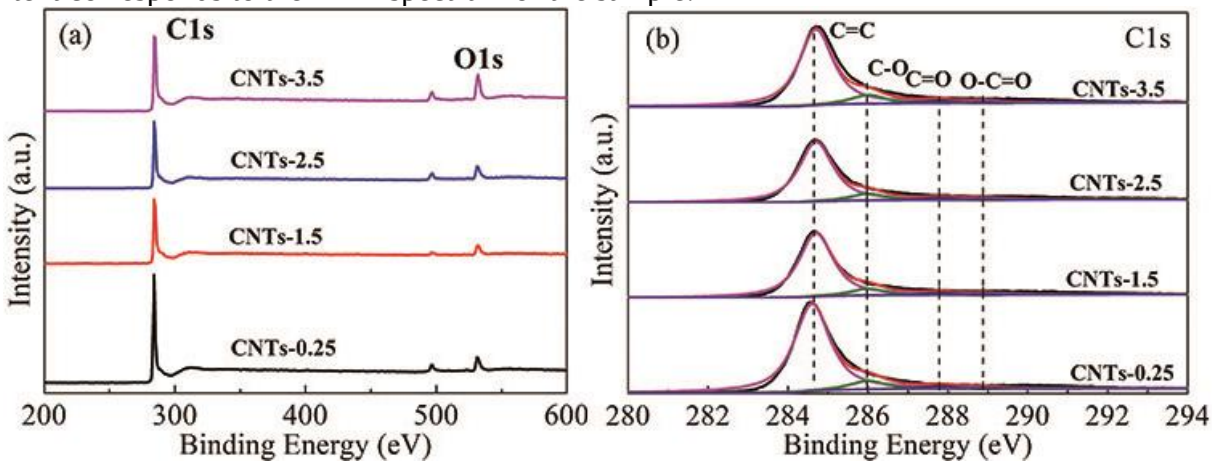

Figure 14: (a) XPS spectra of CNTs prepared at different growth temperatures; (b) C1s spectra of CNTs

Table 3: Contents of C, O, C=C, C-O, C=O, C-C=O of CNTs

samples	C=C	C-O	C=O	C-C=O	C	O
CNTs-0.25	80.26	7.16	1.66	1.60	91.13	8.24
CNTs-1.5	78.45	8.18	2.44	2.34	91.40	7.54
CNTs-2.5	74.87	8.34	2.84	2.63	88.67	10.31
CNTs-3.5	72.68	8.31	2.43	1.98	87.40	13.89

3.4. Optical Performance Analysis

Figure 15 shows the correlation map of the fluorescence properties of the samples. Figure (a) is the PL spectrum of GQDs with different excitation wavelengths (280 ~ 480nm). It can be seen from the Figure that the GQDs sample has a clear emission peak in the blue region of 539nm. Figure (b) is the

PL spectrum of the CNTs-900 sample at the excitation wavelength of 190-220 nm. The results show that there are two strong emission peaks in the ultraviolet band, one at about 362 nm and the other at about 292 nm. near ultraviolet region. Meanwhile, as the excitation wavelength increased from 190 nm to 220 nm, the intensity of the PL peak decreased significantly. Obviously, the energy levels of CNTs are quite different from GQDs, which may be related to the role of carbon nanotubes in the BCNTs-900 sample. Figure 15 (c) shows the PL spectra of pure water, CNTs-700, CNTs-800, and CNTs-900 samples with an excitation wavelength of 200 nm. According to the molecular fluorescence spectroscopy theory , water molecules do not fluoresce. It can be clearly seen from the PL spectrum of pure water in the Figure that as the excitation wavelength increases, it is almost a horizontal line, and no fluorescence is generated. Obviously, all CNTs samples have obvious absorption peaks at 292 nm, 362 nm compared with the emission peaks of graphene quantum dots (539 nm) , which may be related to the higher emission peaks of oxygen-rich graphene quantum dots related to catalytic activity . The photoluminescence of BCNTs is considered to be related to the catalytic activity of GQDs, and the PL emission peak positions of bamboo-shaped carbon nanotubes remain at 292 nm and 362 nm with the change of growth temperature.

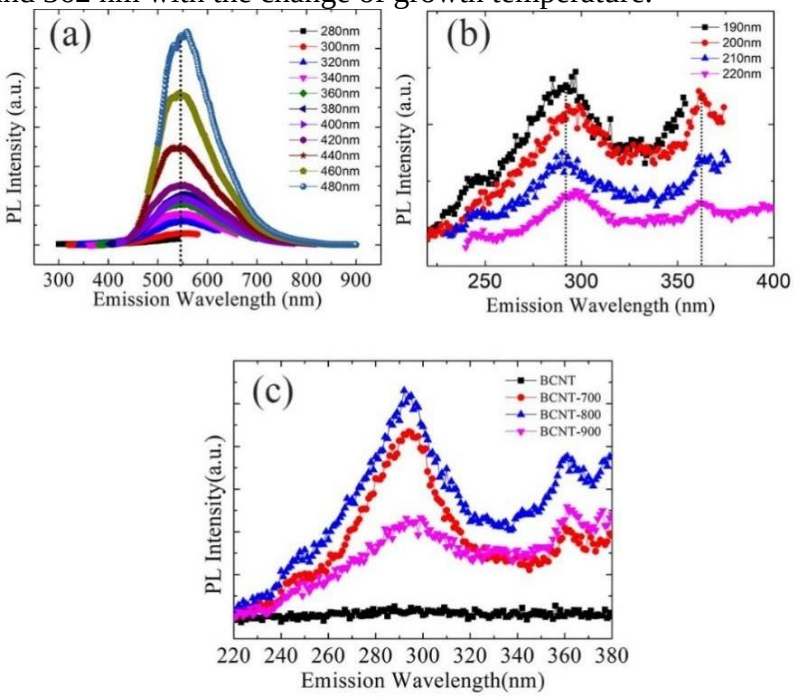

(a) GQDs, (b) BCNTs-900, (c) PL spectra of CNTs samples at 200 nm excitation wavelength

Figure 15: Photoluminescence spectra at different excitation wavelengths:

4. Summary

In this paper, a simple non-catalyzed method to prepare bamboo-shaped carbon nanotubes is introduced, and the factors affecting the morphology and microstructure of carbon nanotubes in the process of preparing carbon nanotubes based on graphene quantum dots and catalyst-free are systematically studied. A study of the optical properties of photoluminescence. Research indicates:

(1) From the comprehensive analysis of SEM results, it can be concluded that when the growth temperature is 900 ℃, it is more suitable for the growth of carbon nanotubes, and the quality of the prepared carbon nanotubes is the best; the growth time has a greater effect on the diameter of the prepared carbon nanotubes. However, the basic morphology of carbon nanotubes will not be changed; the flow rate of acetylene gas has a significant effect on the morphology of the prepared carbon

nanotubes. When the flow rate of acetylene is 0.25 ml/min, the quality of the prepared carbon nanotubes is better.

(2) Within a certain time range, with the increase of growth time and the increase of acetylene flow rate, the diameter of CNTs increased accordingly.

(3) TEM showed that the prepared CNTs were bamboo-type carbon nanotubes; the Raman spectrum and FTIR spectrum of CNTs showed that CNTs contained various oxygen-containing functional groups, and the obtained CNTs were disordered.

(4) PL results show that the BCNTs samples have obvious absorption peaks at 292 nm and 362 nm, and the near-ultraviolet emission of BCNTs is considered to be related to the catalytic activity of GQDs. Therefore, the superior optical properties of CNTs enable them to be used in many applications, including multicolor light-emitting devices, biological applications, and photovoltaic power generation.

Acknowledgment

This work was financially supported by the Natural Science Foundation of Guangxi (No. 2019GXNSFAA24502), the project of improving basic scientific research ability of young and middleaged teachers in Guangxi Universities (2020KY02021). All authors discussed the results and commented on the manuscript. X. Bai and H. Jin contributed equally to this work. All authors discussed the results and commented on the manuscript. H. Yang and Q. Lin are co-corresponding authors contributed equally.

References

[1] Iijima S. (1991) Helical microtubules of graphitic carbon. Nature, , 354, 6348, 56-58.

[2] Novoselov K S, Geim A K, Morozov S V, et al. (2004) Electric field effect in atomically thin carbon films. Science, 306, 5696, 666-669.

[3] Maeda Y, Konno Y, Yamada M, et al. (2018) Control of near infrared photoluminescence properties of single-walled carbon nanotubes by functionalization with dendrons. Nanoscale, 10, 48, 23012-23017.

[4] Shiraki T, Uchimura S, Shiraishi T, et al. (2017) Near infrared photoluminescence modulation by defect site design using aryl isomers in locally functionalized single-walled carbon nanotubes. Chemical Communications, 53, 93, 12544-12547.

[5] Shiraishi T, Shiraki T, Nakashima N. (2017) Substituent effects on the redox states of locally functionalized single-walled carbon nanotubes revealed by in situ photoluminescence spectroelectrochemistry. Nanoscale, 9, 43, 16900.

[6] Sangaraju S, Aharon G. (2006) Generation of hydrophilic, bamboo-shaped multiwalled carbon nanotubes by solid-state pyrolysis and its electrochemical studies. Journal of Physical Chemistry B, 110, 5, 2037-2044.

[7] Singh V, Borkotoky S, Murali A, et al. (2015) Electron paramagnetic resonance and photoluminescence investigation on ultraviolet-emitting gadolinium-ion-doped $CaAl_{12}O_{19}$ phosphors. Spectrochim Acta A Mol Biomol Spectrosc, 139, 1-6.

[8] Hou Z, Krauss T D. (2017) Photoluminescence Brightening of Isolated Single-Walled Carbon Nanotubes. Journal of Physical Chemistry Letters, 8, 19, 4954–4959.

[9] Ishibashi Y, Ito M, Homma Y, et al. (2018) Monitoring the antioxidant effects of catechin using single-walled carbon nanotubes: Comparative analysis by near-infrared absorption and near-infrared photoluminescence. Colloids Surf B Biointerfaces, 161, 139-146.

[10] Liu F, Ming L, Qian F, et al. (2012) Catalyst-free synthesis of reduced graphene oxide–carbon nanotube hybrid materials by acetylene-assisted annealing graphene oxide. Applied Physics Letters, 101, 12, 123107.

[11] Roy-Mayhew J D, Bozym D J, Christian P, et al. (2010) Functionalized graphene as a catalytic counter electrode in dye-sensitized solar cells. ACS nano, 4, 10, 6203-6211.

[12] Rao C N R, Sood A K, Subrahmanyam K S, et al. (2010) Graphene: the new two-dimensional nanomaterial. Angewandte Chemie International Edition, 48, 42, 7752-7777.